Quantitative relationship between polarization differences and the zone-averaged shift photocurrent

Benjamin M. Fregoso, Takahiro Morimoto, and Joel E. Moore

Phys. Rev. B **96**, 075421 — Published 16 August 2017

DOI: 10.1103/PhysRevB.96.075421

The quantitative relationship between polarization differences and the zone-averaged shift photocurrent

Benjamin M. Fregoso,[1] Takahiro Morimoto,[1] and Joel E. Moore[1,2]

[1] *Department of Physics, University of California, Berkeley, California, 94720, USA*
[2] *Materials Sciences Division, Lawrence Berkeley National Laboratory, Berkeley, CA 94720*

A relationship is derived between differences in electric polarization between bands and the "shift vector" that controls part of a material's bulk photocurrent, then demonstrated in several models. Electric polarization has a quantized gauge ambiguity and is normally observed at surfaces via the surface charge density, while shift current is a bulk property and is described by shift vector gauge-invariant at each point in momentum space. They are connected because the same optical transitions that are described in shift currents pick out a relative gauge between valence and conduction bands. We also discuss subtleties arising when there are points at the Brillouin zone where optical transitions are absent. We conclude that two dimensional materials with significant interband polarization differences should have high bulk photocurrent, meaning that the modern theory of polarization can be used as a straightforward way to search for bulk photovoltaic material candidates.

I. INTRODUCTION

Many electronic and optical properties of crystals depend not just on the energy band structure but on the detailed properties of Bloch wavefunctions. A simple example is that optical transitions in a solid, just like in an atom, involve matrix elements that depend on the symmetries of the underlying wavefunctions or orbitals. A deeper example is that the geometric or Berry phase of Bloch wavefunctions controls the electrical polarization and other properties. Although the spontaneous polarization of solids was already of interest to the ancients, and the polarization of a finite distribution of charge density is easily understood, the proper computation of electrical polarization from a unit cell of an infinite crystal had to await the "modern theory of polarization",[1–4] which is now widely used in practical calculations.

The goal of the present work is to explain the quantitative connection between bulk nonlinear optical properties of a material, specifically the shift current piece of photocurrent linear in the intensity of applied light, and electrical polarization. The shift current response is determined by a third rank tensor,

$$J^a_{shift} = 2\sum_b \sigma^{abb} E^b(\omega) E^b(-\omega), \tag{1}$$

where the electric field is $E^b(t) = E^b(\omega)e^{-i\omega t} + E^b(-\omega)e^{i\omega t}$. It is non-vanishing when inversion symmetry is absent, e.g., for ferroelectric materials. The tensor can be written in an intuitive way as (see Appendix A)

$$\sigma^{abb} \approx \frac{e}{\hbar}\sum_{nm}\int_{BZ} R^{a,b}_{nm}\varepsilon^{bb}_{2,nm}, \tag{2}$$

where $\varepsilon^{bb}_{2,nm}(\mathbf{k},\omega)$ is the diagonal (band-resolved) imaginary part of the dielectric function, which is proportional to the density of states, and $\int_{BZ} \equiv \int d\mathbf{k}/(2\pi)^d$ represents an integral over the Brillouin Zone (BZ) in d-dimensions. In the following we often suppress the frequency and momentum dependence of quantities for simplicity of notation. Importantly, the shift current includes a geometrical *shift vector* $R^{a,b}_{nm}$[5–9] defined by,

$$R^{a,b}_{nm} = \frac{\partial \phi^b_{nm}}{\partial k^a} + A^a_{nn} - A^a_{mm}, \tag{3}$$

where A^b_{nm} are the Berry connections

$$A^b_{nm} = i\langle u_n|\frac{\partial}{\partial k^b}|u_m\rangle, \tag{4}$$

and u_n is the periodic part of the Bloch wavefunction at wavevector $\mathbf{k}$. $b = x, y, z$ is a Cartesian axis and ϕ^b_{nm} is the phase of the connection, $A^b_{nm} = |A^b_{nm}|e^{-i\phi^b_{nm}}$. The shift vector also determines the second harmonic generation and electro-optic responses[7,10] of semiconductors.

We note that the definition of shift vector in (3) involves the gauge-dependent quantities A^b_{nn}, A^b_{mm} and ϕ^b_{nm}. However, the combination is gauge-invariant, at all points of the BZ where the optical transition matrix element A^b_{nm} is nonzero. Conversely, electrical polarization is written in the standard theory as an integral of the locally gauge-dependent Berry connection. In other words, the contribution of a particular k-point to the electrical polarization is not meaningfully defined. The total polarization is gauge-dependent up to a quantized ambiguity; in the simplest case of one spatial dimension, the polarization

$$e\int_{BZ} A_{nn} = P_n \tag{5}$$

is defined only up to addition of an integer multiple of electron charge. For example, gauge transformations $u_n \to e^{i\varphi_n}u_n$ change P_n by je, where $j \in \mathbb{Z}$ is the winding number of the angular variable φ_n around the BZ. The physical bulk polarization is defined as a difference with respect to an inversion-symmetric reference system which are adiabatically deformed with each other while keeping a fixed value of j. Nevertheless, the (gauge-invariant) shift vector is directly related in many cases to (gauge-dependent) polarization differences between the valence and conduction band.

The shift current mechanism has recently gained interest for its potential novel optoelectronic applications based on ferroelectrics[11–16]. In particular, 2D materials have highly tunable electronic and optical properties[17–20] and are expected to generate large shift current[21–23]. We can identify three factors that determine the magnitude of the shift current: density of states, velocity matrix elements and shift-vector matrix elements. In three dimensions, they are all intertwined with no obvious relation among them[8]. In two-dimensions, on the other hand, the density of states is constant and the optical transitions are determined by velocity and shift-vector matrix elements. Approximating the dipole matrix elements $|r^b_{nm}|^2$ by a constant ε^{bb} (see Appendix A Eq. A1) we obtain,

$$\sigma^{abb} \approx -\frac{\pi e^3 \varepsilon^{bb}}{\hbar^2} \sum_{nm} \int_{BZ} f_{nm} R^{a,b}_{nm} \delta(\omega_{mn} - \omega), \qquad (6)$$

where $\hbar\omega_{nm} = \hbar\omega_n - \hbar\omega_m$ are band energy differences and $f_{nm} = f_n - f_m$ differences of Fermi distribution functions of band n and m. As pointed out in Ref. 23, in real-life applications such as solar cells, the integrated response over a frequency range is more important than the response at a single frequency. Integrating over all frequency,

$$\int d\omega\ \sigma^{abb} \approx -\frac{\pi e^3 \varepsilon^{bb}}{\hbar^2} \sum_{nm} \int_{BZ} f_{nm} R^{a,b}_{nm}, \qquad (7)$$

we see that the total short circuit current is proportional to the integrated shift vector over the BZ. As shown below, the integral of the shift vector over the BZ is equal to the polarization difference evaluated in a specific gauge; the optical transitions mediated by the shift vector can be viewed as fixing the relative gauge between valence and conduction bands, at least in the simplest case where such transitions are allowed at every k-point.This connection between polarization and shift vector indicates that materials with significant polarization differences between bands (minimized over gauge ambiguities) must have significant shift vectors somewhere in the BZ. In order to understand this relation we consider simple models first.

II. RELATIONSHIP BETWEEN SHIFT VECTOR AND POLARIZATION

We start our analysis focusing on one-dimensional (1D) systems. Let us consider conduction and valence bands, which we label with c and v, separated by an energy gap. In particular, we consider insulators with broken inversion symmetry that support nonzero polarization, where the wavefunctions and off-diagonal Berry connections are complex. In addition, we adopt the periodic gauge[24,25] defined by $\psi_n(k+G, r) = \psi_n(k, r)$ where ψ_n are Bloch wavefunctions and G a reciprocal lattice vector. In this case, all connections A_{nm} are periodic in the BZ, i.e., $A_{cv}(k+G) = A_{cv}(k)$ (see Appendix B). Since the phases

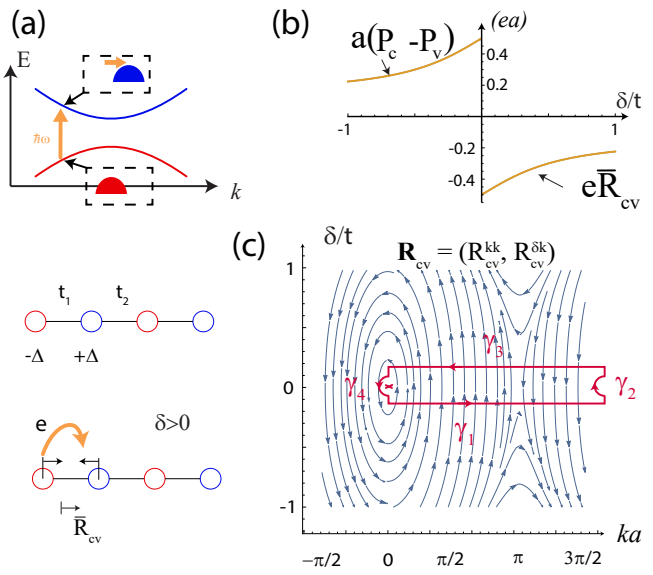

FIG. 1. (a) Top panel, Photoexcitation induces shift of the electron wavepacket in real space. (a) Bottom panel, Rice-Mele (RM) tight-binding model. The unit cell of size a has two sites and alternating hoppings $t_1 = t/2 + \delta/2$ and $t_2 = t/2 - \delta/2$. The distance between conduction and valence band centers is $\bar{R}_{cv}$. For $\delta = 0$, $\bar{R}_{cv} = \pm a/2$, is ambiguous because the system does not break inversion symmetry. For $\delta > 0$, the centers of charge move towards one another by a distance d. The polarization is $P_v(\delta) - P_v(0) = -ed = (\bar{R}_{cv} - a/2)/2$. When a photon is absorbed the electron jumps to another atom a distance $\bar{R}_{cv}$ away. (b) Integral of the shift vector over the BZ and polarization difference. $\bar{R}_{cv}$ has an integer discontinuity at $\delta = 0$. (c) Stream plot of the vector field $\mathbf{R}_{cv} = (R^{kk}_{cv}, R^{k\delta}_{cv})$ which has vortex of charge $+1$ in this *gauge-independent* vector field (see main text). The discontinuity in $\bar{R}_{cv}$ is the charge of the optical zero. In the numerical examples $\Delta > 0$ and $t = e = a = 1$.

ϕ_{cv} at k and $k+G$ coincide modulo 2π, we can define winding W_{cv} of the phase $\phi_{c,v}$ around the BZ as

$$W_{cv} = \frac{1}{2\pi} \oint d\phi_{cv} \in \mathbb{Z}. \qquad (8)$$

Here the winding W_{cv} can be any integer because we still have the freedom to perform transformations such that $\partial_k \varphi_n$ is periodic, e.g., large gauge transformations that change the value of W_{cv} and keep ψ_n periodic over the BZ. We define the *optical gauge* by further constraining the periodic gauge such that $\phi_{cv} = 0$ and constant. When $A_{cv} = 0$ at some k-point in the BZ (which we call "optical zero"), the phase ϕ_{cv} is not well-defined, and hence, W_{cv} is multivalued. The existence of optical zeros is physical and cannot be removed by gauge transformations.

Since R_{cv} is related to the shift of wave packets, we can expect that an integral of R_{cv} over k has a relationship to the difference of polarization of the two bands. Indeed,

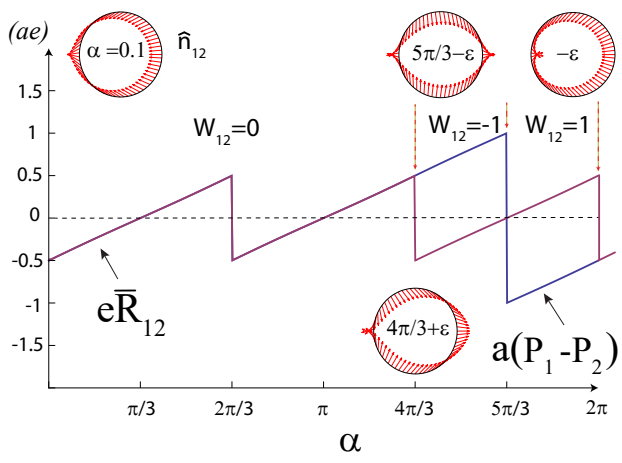

FIG. 2. Polarization and integrated shift vector in a 3-band model, Eq. 13. We find jumps in W_{12} indicating that no single gauge choice gives vanishing winding numbers over the parameter α. $e\bar{R}_{12} = a(P_1 - P_2) + W_{12}ea$ holds for all α. We used parameters $B/A = 0.5, e = a = 1$ and $0 < \varepsilon \ll 1$. In evaluating $P_1 - P_2$, we adopted the gauge given in Eq. E4 with $\varphi_n = 0$.

integrating $R_{cv} = \partial_k \phi_{cv} + A_{cc} - A_{vv}$, leads to

$$e\bar{R}_{cv} = ea \int_{BZ} R_{cv} = eaW_{cv} + aP_c - aP_v, \qquad (9)$$

where $P_{c,v}$ is polarization of conduction and valence bands. Eq. 9 shows that the integral of the shift vector over the BZ is proportional to the polarization difference between the conduction and valence bands up to an integer W_{cv}. In particular, the optical gauge allows us to directly connect shift vector and polarization as

$$e\bar{R}_{cv} = aP_c - aP_v \qquad (10)$$

since $W_{cv} = 0$. We emphasize that this is only possible when there is no optical zero in the region of the integral. Let us consider some explicit examples.

III. RICE-MELE MODEL

Let us apply the above analysis to the Rice-Mele (RM) model[26], which is an archetypal model of ferroelectricity along the polar axis. It applies to Polyacetylene, $BaTiO_3$ and even monochalcogenides[23]. It is given by

$$\hat{H} = \sum_i [(\frac{t}{2} + (-1)^i \frac{\delta}{2}) c_i^\dagger c_{i+1} + h.c. + (-1)^i \Delta c_i^\dagger c_i]. \qquad (11)$$

The c_i ($c_i^\dagger$), annihilates (creates) s-wave electron states at site i. The unit cell of size a has two sites, δ parametrizes the dimerization of the chain and Δ the staggered on-site potential, Fig. 1a. Inversion symmetry is broken if $\Delta \neq 0$ and $\delta \neq 0$, and preserved otherwise (for details of the model, see Appendix D). The shift vector for this (and any two-band) model can be computed and studied analytically. For example its gauge invariance is made apparent when we write it in terms of the Hamiltonian and its derivatives (see Appendix C).

With a gauge in Eq. D3, we obtain $W_{cv} = 0$ (see Fig. 1(b)). The shift vector R_{cv} is usually assigned the meaning of the size of the microscopic dipole formed by the photo excited particle-hole[5]. Since, R_{cv} could grow without limit (see Appendix D), we believe, $\bar{R}_{cv}$ has a more well defined physical meaning, namely, as the the distance between the valence and conduction centers of charge (Fig. 1a), and is therefore bounded by the lattice spacing a.

At $(ka, \delta) = (0, 0)$ we have $A_{cv} = 0$ and the size of the discontinuity in $\bar{R}_{cv}$ (Fig. 1(b)) is determined by the vorticity associated with the optical zero as follows. We consider the parameter δ as if it were a Cartesian direction and define the gauge invariant shift vectors as $R^{\mu\nu}_{cv} = \partial_\mu \phi^\nu_{cv} + A^\mu_{cc} - A^\mu_{vv}$ with $\mu, \nu = ka, \delta$. The singularity at the optical zero is clear in the vector field $\mathbf{R}_{cv} = (R^{kk}_{cv}, R^{\delta k}_{cv})$ shown in Fig. 1(c). At the optical zero, the shift vector diverges (for details, see Appendix D). The jump in $\bar{R}^{kk}_{cv} (= \bar{R}_{cv})$ at $\delta = 0$ is obtained from the integral of $\mathbf{R}_{cv}$ along the path $\gamma = \sum_{n=1}^4 \gamma_n$ described in Fig. 1(c), which leads to

$$\frac{1}{2\pi} \oint_{\gamma_2 \gamma_4 \to 0} d\lambda \cdot \mathbf{R}_{cv} = \frac{\bar{R}_{cv}(0^-) - \bar{R}_{cv}(0^+)}{a} = 1, \qquad (12)$$

with $d\lambda \equiv (dk, d\delta)$. One can check that the vortex at $(ka, \delta) = (\pi, 0)$ does not contribute to the path integral since $\mathbf{R}_{cv}$ vanishes at this point. Furthermore, this vortex structure at optical zeros governs the charge pumping induced by a periodic change of parameter [e.g., over a path $(\Delta, \delta) = (\cos\theta, \sin\theta)$ with $\theta = 0 \to 2\pi$]. The pumped charge in this circuit is given by "the Berry curvature" as $\int_S \Omega^{cv}_{\mu\nu}$ with $\Omega^{cv}_{\mu\nu} = \partial_\mu R^{\mu k}_{cv} - \partial_\nu R^{\nu k}_{cv}$.

IV. 1D 3-BAND MODEL WITH INVERSION BREAKING

Next we show that the direct relationship between shift vector and polarization is not limited to the two band models by demonstrating the relationship in the case of general number of bands. As an example, we consider the 3-band model described by

$$\hat{H} = \sum_j t_j c_j^\dagger c_{j+1} + h.c., \qquad (13)$$

with $t_j = A + B\cos(2\pi j/3 - \alpha)$. In this model the lower band pumps $-2e$ while the other two pump e per cycle in $\alpha \in [0, 2\pi]$. (For details of the model see Appendix E) To be concrete, let us consider the lowest two bands $n = 1, 2$. As can be seen from Fig. 2. $\bar{R}_{12}$ has integer discontinuities at the values of α for which $A_{12} = 0$ and ϕ_{12} is not

well defined. The exact location of the discontinuities is determined by the vorticity of the field $\mathbf{R}_{12}$ and whether it vanishes or not, see Appendix E.

V. TWO AND THREE DIMENSIONS

We have shown in detail how the integral of the shift vector is related to the electric polarization differences in 1D. We next consider generalizations to higher dimensional. In higher dimensions the shift vector has two or more Cartesian indices $a, b = x, y, z$. The analogous definition to Eq. 8 is,

$$W^{a,b}_{nm} = \frac{v}{l^a}\int_{BZ} \frac{\partial \phi^b_{nm}}{\partial k^a}, \tag{14}$$

where l^a is the primitive lattice vector component and v is the volume of the primitive unit cell. If we defined the integral of shift vector over the BZ as

$$\bar{R}^{a,b}_{nm} = v\int_{BZ} R^{a,b}_{nm}. \tag{15}$$

then we obtain

$$e\bar{R}^{a,b}_{nm} = v(P^a_n - P^a_m) + W^{a,b}_{nm} v Q^a, \tag{16}$$

where $Q^a = el^a/v$ is the quantum of polarization along the a Cartesian axis. There are two situations of interest. First, if there are no optical zeros on the parameter space path, we can define an optical gauge where the polarization difference can be inferred from the integral of the shift vector with $W^{a,b}_{nm} = 0$. In this case, $e\bar{R}^{a,b}_{nm} = v(P^a_n - P^a_m)$ holds and materials with large polarization differences (the right hand side) lead to efficient photovoltaic responses (through shift vector in the left hand side).

Second, if there exist optical zeros, the optical gauge has discontinuities. Here, W^{ab}_{nm} is not quantized since a winding number $\int dk_a \partial_{k_a}\phi^b_{nm}$ as a function of k_c ($c \neq a$) in general has jumps at optical zeros. In this case, while we cannot directly relate $\bar{R}^{a,b}_{nm}$ and $P^a_n - P^a_m$, the right hand side including $W^{a,b}_{nm}$ can be evaluated in a fairly easy way, providing a guideline to search efficient photovoltaic materials. In particular, Eq. 16 shows that the polarization difference and locations of optical zeros (that determine $W^{a,b}_{nm}$) are important in understanding photovoltaic responses in the left hand side.

As an example, consider a simple extension of the RM model to two-dimensions. It consists of two 1D RM models, one in the x-direction and the other in the y-direction, with dimerization parameters, δ_x, δ_y. We suppose that the staggered potential is modulated along x but constant along y. It is easy to show that the electrical polarization is along x and only transitions from bands $1 \to 3$ and $2 \to 4$ are allowed. There is a line of optical zeros at $(k_x, k_y, \delta_x) = (0, k_y, 0)$ for all k_y and one can define gauge-invariant fields in the plane (k_x, δ_x) with similar vorticity as in Fig. 1(c). As long as $\delta_x \neq 0$ the winding $W^{xx}_{12} = 0$. Similarly to the RM model in 1D, the existence of the singularity at $\delta_x = 0$ gives rise to a discontinuity of $\bar{R}^{xx}_{12}$.

VI. DISCUSSION AND CONCLUSIONS

We demonstrated that the integral of the shift vector is a dominant factor in determining the total shift current generated in 2D materials. Barring points where the optical transitions are forbidden, the integral of the shift vector has the meaning of polarization differences between conduction and valence bands. We also describe the theoretical tools for analyzing the polarization differences in the presence or absence of optical zeros.

With the caveats explained above, Eq. 7 gives,

$$\int d\omega\ \sigma^{aaa} \approx -\frac{\pi e^2 \varepsilon^{aa}}{\hbar^2}\sum_{nm} f_{nm}(P^a_n - P^a_m), \tag{17}$$

where we assumed the optical gauge and $f_{nm} = -1$ for $n(m)$ a conduction (valence) band and 1 when $n(m)$ a valence(conduction) band. The short-circuit current on a device is proportional the sum of polarization differences. Since the electronic part of the spontaneous polarization is the sum over all occupied (valence) band polarizations. Eq. 17 suggests that 2D ferroelectrics are natural candidates for materials with large shift current generation. Hence, our results provide the long-sought link between electric polarization and shift current injection.

There is numerical evidence that 2D ferroelectric single-layer IV-monochalcogenides have large shift current [22,23]. A recent experiment measuring shift current on thin films of GeS is consistent with our results[27]. We also expect large shift current in the recently discovered 2D ferroelectric SnTe[28]. Finally, the right-hand side of Eq. 16 is easier to evaluate than the left-hand side with with standard ab-initio methods and serves as an estimate of shift current generation, and provide a practical guideline to search for materials with large shift currents.

VII. ACKNOWLEDGMENTS

We thank F. de Juan, M. Kolodrubetz and S. Barraza-Lopez for useful discussions. BMF acknowledges support from AFOSR MURI, Conacyt and NERSC contract No. DE-AC02-05CH11231. TM acknowledges support from the Gordon and Betty Moore Foundation's EPiQS Initiative Theory Center Grant. JEM acknowledges funding from NSF DMR-1507141 and a Simons Investigatorship.

Appendix A: Phase-independent expression of shift vector

The shift current tensor, Eq. 2 in main text, in d-dimension is usually written as[7],

$$\sigma^{abc}(0;\omega,-\omega)=\frac{i\pi e^3}{2\hbar^2}\int_{BZ}\sum_{nm}f_{nm}(r^b_{mn}r^c_{nm;a}+r^c_{mn}r^b_{nm;a})\delta(\omega_{mn}-\omega), \quad \text{(A1)}$$

Here we defined the integral as $\int_{BZ}\equiv\int d\mathbf{k}/(2\pi)^d$ over the Brillouin Zone (BZ) in d-dimensions for notational convenience. $\hbar\omega_{nm}=\hbar\omega_n-\hbar\omega_m$ are band energy differences and $f_{nm}=f_n-f_m$ differences of Fermi distribution functions of band n and m. The dipole matrix elements r^a_{nm} and generalized derivatives are

$$r^b_{nm}\equiv A^b_{nm}\quad [n\neq m \text{ and } 0 \text{ otherwise}] \quad \text{(A2)}$$

$$r^b_{nm;a}\equiv\frac{\partial r^b_{nm}}{\partial k^a}-i(A^a_{nn}-A^a_{mm})r^b_{nm}. \quad \text{(A3)}$$

$A^b_{nm}=i\langle u_n|\frac{\partial}{\partial k^b}|u_m\rangle$ are the Berry connections, $\hbar\omega_{nm}=\hbar\omega_n-\hbar\omega_m$ are the band energies and $f_{nm}=f_n-f_m$ are the fermionic occupation numbers. We can write $A^b_{nm}=v_{nm}/i\omega_{nm}$, for non-degenerate bands where v^b_{nm} is the velocity matrix element. Setting $b=c$ for linear polarization and using polar representation, $r^a_{nm}=|r^a_{nm}|e^{-i\phi^a_{nm}}$, Eq. A1 reduces to,

$$\sigma^{abb}(0;\omega,-\omega)=-\frac{\pi e^3}{\hbar^2}\int_{BZ}\sum_{nm}f_{nm}R^{a,b}_{nm}|r^b_{nm}|^2\times\delta(\omega_{mn}-\omega), \quad \text{(A4)}$$

where $R^{a,b}_{nm}$ is the so-called shift 'vector',

$$R^{a,b}_{nm}=\frac{\partial\phi^b_{nm}}{\partial k^a}+A^a_{nn}-A^a_{mm}, \quad \text{(A5)}$$

An alternative expression for the shift vector, which avoids the use of ϕ^b_{nm}, can be obtained from Eq. A1. Since $\sigma_2(0;\omega,-\omega)$ is real we have

$$R^{a,b}_{nm}|r^b_{nm}|^2=-\mathrm{Im}\big[r^b_{mn}r^b_{nm;a}\big]. \quad \text{(A6)}$$

The right-hand-side is gauge invariant and has simple analytical expressions for effective models of monochalcogenides[22,23]. It contains two important physical effects, density of states and the geometry of Bloch wavefunctions. To disentangle these effects, let us consider the case where $r^b_{nm}\neq 0$ (equivalently $v^b_{nm}\neq 0$) then the shift vector itself is well defined,

$$R^{a,b}_{nm}=-\frac{1}{|r^b_{nm}|^2}\mathrm{Im}\big[r^b_{mn}r^b_{nm;a}\big], \quad \text{(A7)}$$

and independent of the density of states. In the independent-particle approximation, the imaginary part of the dielectric function,

$$\frac{\varepsilon^{ab}_2(\omega)}{\varepsilon_0}=\delta_{ab}-\frac{e^2\pi}{\varepsilon_0\hbar}\int_{BZ}\sum_{nm}f_{nm}r^a_{nm}r^b_{mn}\delta(\omega_{mn}-\omega). \quad \text{(A8)}$$

is dominated by the second term and comparing with Eq. A4 we obtain Eq. 2 in the main text.

Appendix B: The optical gauge

The solutions of the Schrodinger equation with a periodic potential are Bloch wavefunctions,

$$\psi_n(\mathbf{k},\mathbf{r})=e^{i\mathbf{k}\cdot\mathbf{r}}u_n(\mathbf{k},\mathbf{r}), \quad \text{(B1)}$$

Where n is the bands index and $\mathbf{k}$ the crystal momentum. $u_n(\mathbf{k},\mathbf{r}+\mathbf{R})=u_n(\mathbf{k},\mathbf{r})$ is the cell periodic part of the wave function and $\mathbf{R}$ is a lattice vector. The solutions of the Schrodinger equation are invariant under phase transformations ($U(1)$ gauge transformations),

$$\psi'_n(\mathbf{k},\mathbf{r})=e^{i\varphi_n(\mathbf{k})}\psi_n(\mathbf{k},\mathbf{r}). \quad \text{(B2)}$$

Under a gauge transformations the Berry connections transforms as

$$A'^b_{nm}=A^b_{nm}e^{i(\varphi_m-\varphi_n)} \quad \text{(B3)}$$

$$A'^b_{mm}=A^b_{mm}-\frac{\partial\varphi_m(\mathbf{k})}{\partial k^b}. \quad \text{(B4)}$$

The diagonal matrix elements can change by an arbitrary phase φ_n. Hence choosing the diagonal elements is equivalent to fixing a particular gauge. On the other hand, the off diagonal Berry connections transform as operators and therefore, if $A^b_{nm}=0$ in one gauge it vanishes in all gauges; The dipole matrix elements and its generalized derivatives, transform as operators

$$r'^b_{nm}=e^{i(\varphi_m-\varphi_n)}\,r^b_{nm} \quad \text{(B5)}$$

$$r'^b_{nm;a}=e^{i(\varphi_m-\varphi_n)}\,r^b_{nm;a}. \quad \text{(B6)}$$

but the standard derivative $\partial r^b_{nm}/\partial k^a$ does not transform as a tensor. From these results we see that shift vector, Eqn. A7, is gauge invariant.

Now, the Bloch states at $\mathbf{k}$ and $\mathbf{k}+\mathbf{G}$, with $\mathbf{G}$ a reciprocal lattice vector, are physically equivalent states. The can differ at most by a phase λ,

$$\psi_n(\mathbf{k}+\mathbf{G})=\lambda_n\psi_n(\mathbf{k}), \quad \text{(B7)}$$

where $\lambda_n=e^{i\theta_n(\mathbf{k},\mathbf{G})}$ is determined by the choice of φ_n. For arbitrary λ_n the connections at $\mathbf{k}$ and $\mathbf{k}+\mathbf{G}$ are related as,

$$A^b_{mm}(\mathbf{k}+\mathbf{G})=A^b_{mm}(\mathbf{k})+\lambda^*_m i\frac{\partial\lambda_m}{\partial k^b} \quad \text{(B8)}$$

$$A^b_{nm}(\mathbf{k}+\mathbf{G})=\lambda^*_n\lambda_m A^b_{nm}(\mathbf{k}). \quad \text{(B9)}$$

In general, the off diagonal elements at $\mathbf{k}$ and $\mathbf{k}+\mathbf{G}$ differ by an arbitrary phase, but if we choose the periodic gauge where $\lambda_n=1$, then both the Bloch wavefunctions and connections (diagonal *and* off-diagonal) are

periodic. Note that the phases at $\mathbf{k}$ and $\mathbf{k}+\mathbf{G}$ may differ by and integer multiple of 2π. The ambiguity in A^b_{nn} gives rise the an integer ambiguity in the polarization and the ambiguity in A^b_{nm} to the interband winding number $W^{b,b}_{nm}$ described in the main text. This is because we still have freedom to impose gauge transformations in which $\nabla_{\mathbf{k}}\varphi(\mathbf{k})$ is periodic[25], which include large gauge transformations. Let us call the subset with $W^{a,b}_{nm}=0$ the optical gauge.

Appendix C: Shift vector of two-band model from Hamiltonian derivatives

For a two-band Hamiltonian given in first quantization as $H=\sum_i d_i\sigma^i$, where $\mathbf{d}=(d_x,d_y,d_z)$, the right-hand side of Eq. A6 is,

$$\mathrm{Im}\big[r^b_{12}r^b_{21;a}\big]=\epsilon_{mij}\frac{1}{4E^5}\big(d_m d_{i,a}d_{j,b}d_l d_{l,a} - E^2 d_m d_{i,a}d_{j,ab}\big) \quad \text{(C1)}$$

$\pm E(\mathbf{k})$ are the eigenvalues of the Bloch Hamiltonian, and $d_{i,a}=\partial d_i/\partial k^a$. This result is easier to obtain by expanding both sides of the identity $\partial_{k^b}\partial_{k^a}\langle u_n|H|u_m\rangle = \delta_{nm}\partial_{k^b}\partial_{k^a}E_n$. From this we obtain an expression for the generalized derivative in terms of velocity matrix elements only[7,22], $(n\neq m)$

$$r^a_{nm;b}=-\frac{1}{i\omega_{nm}}\left[\frac{v^a_{nm}\Delta^b_{nm}+v^b_{nm}\Delta^a_{nm}}{\omega_{nm}}-w^{ab}_{nm} + \sum_{p\neq n,m}\Big(\frac{v^a_{np}v^b_{pm}}{\omega_{pm}}-\frac{v^b_{np}v^a_{pm}}{\omega_{np}}\Big)\right], \quad \text{(C2)}$$

where $v^b_{nm}=\langle n|\partial_{k_b}H|m\rangle$ are the velocity matrix elements, $\Delta^b_{nm}=v^b_{nn}-v^b_{mm}$, $w^{ba}_{nm}=\langle n|\partial_{k_b}\partial_{k_a}H|m\rangle$ and $\hbar\omega_{nm}=E_n-E_m$. In the evaluation, we used various standard identities. Note the extra term w^{ab}_{nm} compared to Ref.[7], where $H=p^2/2m+V(x)$ and $w^{ab}_{nm}=\delta_{nm}\delta^{ab}/m$ is diagonal. Tight-binding models are, of course, approximations to real-life solid state Hamiltonians and comparison with experiments must proceed with caution to avoid spurious terms arising from the use of a tight-binding models. r^b_{nm} can also be obtained in terms of Hamiltonian derivatives. Recall that by definition only off-diagonal terms contribute,

$$|r^b_{12}|^2=\frac{1}{4E^2(E^2-d_z^2)}\big[(d_zE_{,b}-d_{z,b}E)^2 + (d_xd_{y,b}-d_{x,b}d_y)^2\big]. \quad \text{(C3)}$$

Hence the shift vector written as,

$$R^{a,b}_{12}=-\epsilon_{mij}\frac{(E^2-d_z^2)(d_m d_{i,a}d_{j,b}d_l d_{l,a}-E^2 d_m d_{i,a}d_{j,ab})}{E^3\big[(d_zE_{,b}-d_{z,b}E)^2+(d_xd_{y,b}-d_{x,b}d_y)^2\big]}, \quad \text{(C4)}$$

is explicitly gauge-independent. In particular, the expression for the shift vector for $b=a$ reduces to

$$R^{a,a}_{cv}=-\frac{|\mathbf{d}|\mathbf{d}\cdot(\mathbf{d}'\times\mathbf{d}'')}{|\mathbf{d}|^2|\mathbf{d}'|^2-(\partial_{k^a}|\mathbf{d}|^2)^2/4}, \quad \text{(C5)}$$

where $d'_i=\partial_{k^a}d_i$.

Appendix D: Shift vector and current in Rice-Mele model

In this section the shift vector and shift current for the Rice-Mele model of ferroelectrics is computed. The Hamiltonian is

$$\hat{H}_{RM}=\sum_i[(\frac{t}{2}+(-1)^i\frac{\delta}{2})(c^\dagger_i c_{i+1}+h.c.)+(-1)^i\Delta c^\dagger_i c_i], \quad \text{(D1)}$$

where $c_i(c^\dagger_i)$, destroys(creates) electron states at site i, δ parametrizes the dimerization of the chain and Δ the staggered potential on sites A and B. If $\Delta\neq 0$, and $\delta\neq 0$ inversion symmetry is broken. The unit cell (of length a) has two sites. We obtain the Bloch Hamiltonian,

$$H_{RM}=\sum_i d_i\sigma_i=\sigma_x\ t\cos ka/2-\sigma_y\ \delta\sin ka/2+\sigma_z\ \Delta \quad \text{(D2)}$$

and eigenfunctions,

$$u_c=\frac{e^{i\varphi_c}}{\sqrt{2}}\begin{pmatrix}v\\ue^{i\phi}\end{pmatrix} \qquad u_v=\frac{e^{i\varphi_v}}{\sqrt{2}}\begin{pmatrix}u\\-ve^{i\phi}\end{pmatrix}, \quad \text{(D3)}$$

where $H_{RM}u_{c,v}=\pm Eu_{c,v}$, $\phi=\arctan[(-\delta/t)\tan(ka/2)]$ (mod π) is the azimuthal angle of the vector H_{RM} in the Bloch sphere, $u=\sqrt{1-\Delta/E}$, $v=\sqrt{1+\Delta/E}$ and the eigenvalues are given by $E=(t^2\cos^2 ka/2+\delta^2\sin^2 ka/2+\Delta^2)^{1/2}$ for the conduction and $-E$ for the valence band (ϕ should not be confused with ϕ_{cv}). We have added a gauge dependence φ_n, $(n=c,v)$. The Berry connection will depend explicitly on the gauge used but results on the shift vector/current are gauge independent. In this section we choose $\partial_k\varphi_n=0$. The Bloch wavefunctions are $\psi_n(k,r)=\sum_j e^{ikaj}[u^A_n(k)\chi(r-aj)+e^{ika/2}u^B_n(k)\chi(r-aj-a/2)]$, where χ are the atomic wavefunctions and $u^{A,B}_n$ projections of the eigenfunctions on site A(B). The Berry connections,

$$A_{nn}=iu^\dagger_n\partial_k u_n=\frac{at\delta(E\mp\Delta)}{4E(E^2-\Delta^2)} \quad (n=c,v) \quad \text{(D4)}$$

$$A_{cv}=iu^\dagger_c\partial_k u_v=\frac{a\ ie^{-i(\varphi_v-\varphi_c)}}{8E^2\sqrt{E^2-\Delta^2}}\big[\Delta(t^2-\delta^2)\sin ka + 2i\delta tE\big], \quad \text{(D5)}$$

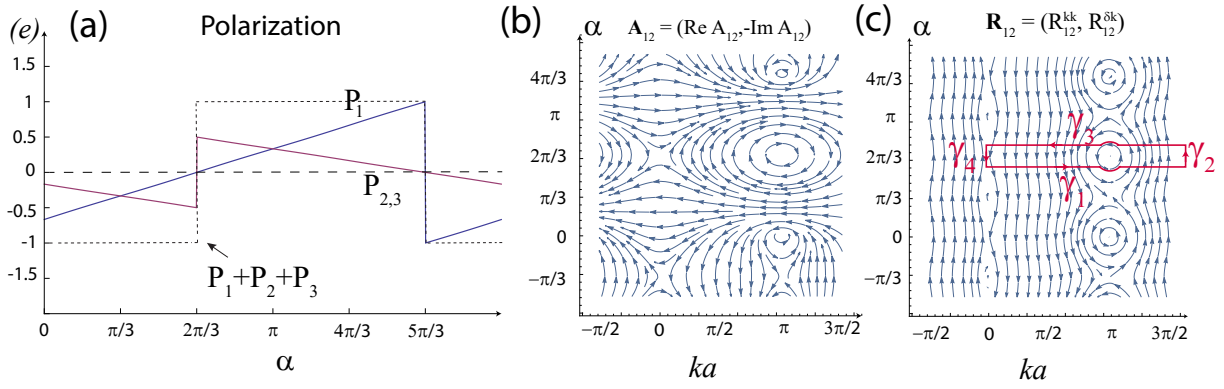

FIG. 3. Color online. (a) polarizations of each band of model Eq. E1 as a function of α. (b) W_{12} changes at optical zeros $\alpha = 0, 4\pi/3$ and at the inversion symmetric point $\alpha = 5\pi/3$. (c) gauge-invariant field $(R^{kk}_{12}, R^{\delta k}_{12})$ showing the vorticity of the optical zeros giving the discontinuities of $\bar{R}_{12}$. The loop $\gamma = \sum_n \gamma_n$ encloses a vortex of charge $+1$, (see main text). One can check that $\mathbf{R}_{12} = 0$ at $ka = 0$, and hence it does not contribute to the path integral. We chose units such that $e = a = 1$

are both periodic with period $2\pi/a$. We define the phase ϕ_{cv} by $A_{cv} = |A_{cv}|e^{-i\phi_{cv}} = |A_{cv}|(\cos\phi_{cv}, -\sin\phi_{cv})$, and its derivative is,

$$\partial_k\phi_{cv} = \frac{\Delta}{2E}\frac{a\delta t(\delta^2-t^2)\left[4E^2\cos ka + (t^2-\delta^2)\sin^2 ka\right]}{\left[\Delta^2(\delta^2-t^2)^2\sin^2 ka + 4\delta^2t^2E^2\right]}. \tag{D6}$$

This expression is smooth for $\delta \neq 0$. If $\delta = 0$ it can be seen that $A_{cv} = 0$ at $ka = 0, \pi$. The shift vector, $R_{cv} = \partial_k\phi_{cv} + A_{cc} - A_{vv}$, can be computed analytically as,

$$R_{cv} = \frac{\Delta}{2E}\frac{a\delta t(\delta^2-t^2)\left[4E^2\cos ka + (t^2-\delta^2)\sin^2 ka\right]}{\left[\Delta^2(\delta^2-t^2)^2\sin^2 ka + 4\delta^2t^2E^2\right]} - \frac{\Delta}{2E}\frac{at\delta}{(E^2-\Delta^2)}. \tag{D7}$$

Some observations about the behavior of the shift vector in the RM model are in order, (a) Generally, the shift vector does not vanish; (b) The shift vector is peaked at $ka = 0$ or $ka = \pi$, and (c) The shift vector can exceed the lattice spacing a. To illustrate this consider some limiting values of the shift vector,

$$R_{cv}\big|_{\lim\ k\to 0} = -\frac{at\Delta}{2\delta\sqrt{t^2+\Delta^2}}\Big|_{\lim\ \delta\to 0} = \infty \tag{D8}$$

$$R_{cv}\big|_{\lim\ k\to \pi/a} = -\frac{a\delta\Delta}{2t\sqrt{\delta^2+\Delta^2}}\Big|_{\lim\ \delta\to 0} = 0 \tag{D9}$$

$$R_{cv}\big|_{\lim\ \delta\to t} = -\frac{a\Delta}{2\sqrt{t^2+\Delta^2}}\Big|_{\lim\ \Delta\to 0} = -a\Delta/2t \quad \text{(flat band limit)}. \tag{D10}$$

Hence one can check that at $ka = \pi$ the field $\mathbf{R}_{cv} = (R^{kk}_{cv}, R^{\delta k}_{cv})$, defined in the main text, vanishes and at $ka = 0$ it diverges.

Shift current.- If the electric field is along the chain, e.g., the z-direction, the shift current is

$$J^z_{\rm shift}(\omega) = 2\sigma^{zzz}(0;\omega,-\omega)E^z(\omega)E^z(-\omega). \tag{D11}$$

For the two-band model this reduces to

$$\sigma^{zzz}(0;\omega,-\omega) = e^3\int_0^{2\pi/a} dk \frac{|\langle u_c|v^z|u_v\rangle|^2 R_{cv}}{\hbar^2\omega^2}\delta(\frac{2E}{\hbar}-\omega) \tag{D12}$$

where the matrix elements of the velocity operator $v^z = \hbar^{-1}\partial H_{RM}/\partial k$ are

$$|\langle u_c|v^z|u_v\rangle|^2 = \frac{a^2}{16\hbar^2}\frac{1}{E^2(E^2-\Delta^2)}\left(\Delta^2(t^2-\delta^2)^2\sin^2 ka + 4t^2\delta^2E^2\right). \tag{D13}$$

The shift vector and the matrix elements of the velocity each have complicated expressions but the combination (the 'integrand'),

$$\frac{\hbar^2|v^z_{cv}|^2}{4E^2}R_{cv} = |r^z_{cv}|^2R_{cv} = -{\rm Im}[r^z_{cv}r^z_{vc;z}] \tag{D14}$$

is simply,

$${\rm Im}[r^z_{cv}r^z_{vc;z}] = \frac{a^3t\delta\Delta}{32E^3}. \tag{D15}$$

For $\delta \ll \Delta$, R_{cv} is sharply peaked at $ka = 0$ but $|r^z_{cv}|$ peaks at $ka = \pi$. As δ increases the peak in R_{cv} and $|r^z_{cv}|^2$ broadens but their peaks maximum also decreases. The dependence on the velocity matrix elements (imaginary part of the dielectric function) is very prominent here because the system is 1D. The analytical expression for the shift current of the RM model simplifies to

$$\sigma^{zzz}(0;\omega,-\omega) = -\frac{e^3a^3t\delta\Delta}{8\hbar^4\omega^3}\sum_i\frac{1}{|\partial_kE(k_i)|}, \tag{D16}$$

where $\partial_kE = a(\delta^2-t^2)\sin ka/4E$ is the velocity at momentum k and k_i are the two solutions of $2E(k_i) = \hbar\omega$ for $\hbar\omega > 2E$. In 1D, σ^{zzz} diverges as $\omega^{-3}(2E-\hbar\omega)^{-1/2}$ at the band edge, but is suppressed in 2D, where the role of the shift vector becomes prominent.

Appendix E: Polarization and shift vector in a 3-band model

Let us consider the 1D model Hamiltonian

$$\hat{H}_{3B} = \sum_j t_j c_j^\dagger c_{j+1} + h.c., \tag{E1}$$

with $t_j = A + B\cos\left(2\pi j/3 - \alpha\right)$. There are tree distinct values of the hoppings $t_j = t_1, t_2, t_3$. Hence, the unit cell (of size a) has 3 nonequivalent sites. The crystal has inversion symmetry for $\alpha = 0, \pi/3, 2\pi/3, \pi, 4\pi/3, 5\pi/3$, when two of the hopping are equal. The Bloch Hamiltonian is,

$$H_{3B} = \begin{bmatrix} 0 & t_1 e^{ika/3} & t_3 e^{-ika/3} \\ t_1 e^{-ika/3} & 0 & t_2 e^{ika/3} \\ t_3 e^{ika/3} & t_2 e^{-ika/3} & 0 \end{bmatrix}. \tag{E2}$$

The eigenvalues and eigenvectors, $H_{3B}u_n = E_n u_n$, are

$$E_n = 2t_r \cos\big(\frac{1}{3}\arccos\left(t_g^3\cos\left(ka\right)/t_r^3\right) - \frac{2\pi n}{3}\big), \tag{E3}$$

where $(n = 1, 2, 3)$ and we defined the root mean square and geometric average $t_r = \sqrt{(t_1^2 + t_2^2 + t_3^2)/3}$ and $t_g = (t_1 t_2 t_3)^{1/3}$ respectively, and

$$u_n = \frac{e^{i\varphi_n}}{N_n}\begin{bmatrix} E_n^2 - t_2^2 \\ t_2 t_3 e^{2ika/3} + E_n t_1 e^{-ika/3} \\ t_2 t_1 e^{-2ika/3} + E_n t_3 e^{ika/3} \end{bmatrix}, \tag{E4}$$

where φ_n is chosen to enforce the periodic gauge. The normalization is $N_n = [(E_n^2 - t_2^2)^2 + (t_2^2 - E_n^2)(t_3^2 - E_n^2) + (t_1^2 - E_n^2)(t_2^2 - E_n^2)]^{1/2}$. Using these wave functions, the Berry connections are calculated analytically as,

$$\begin{aligned} A_{nn} &= \frac{a}{2N_n^2}(E_n^2 + 2t_2^2)(t_1^2 - t_3^2) \\ &\quad - \frac{i}{N_n^2}\left[3E_n(\partial_k E_n)(E_n^2 - t_r^2) + 2aE_n t_g^3 \sin\left(ka\right)\right] \end{aligned} \tag{E5}$$

$$\begin{aligned} A_{nm} &= \frac{a}{3N_n N_m}(E_n E_m + 2t_2^2)(t_1^2 - t_3^2) \\ &\quad + \frac{i2at_g^3(E_n^2 + E_m^2 + E_n E_m - 3t_2^2)\sin\left(ka\right)}{3N_n N_m(E_n - E_m)}. \end{aligned} \tag{E6}$$

Note that the Berry connections are periodic in k-space with period $G = 2\pi/a$. One can check that the optical zeros of A_{12} are $\alpha = 0, 2\pi/3, 4\pi/3$, where $A_{12}(ka = \pi, \alpha)$ vanishes and hence the phase of ϕ_{12} is not well defined. In fig. 3(a,b) we show the windings of the interband connection A_{12} and the gauge-invariant vorticity of the optical zeros in the field $\mathbf{R}_{12}$ described in the main text.

Polarization.- The polarization is given by the integral over the Berry connection as

$$P_n(\alpha) = \frac{1}{2\pi}\int dk A_{nn}(k, \alpha) \tag{E7}$$

In Fig. 3a we show the individual band polarizations as a function of α. Note that the sum $P_1 + P_2 + P_3 = \pm 1 \pmod e$, as expected. Also, the total charge pumped of band n per cycle is

$$\begin{aligned} c_n(\alpha) &= \int_0^\alpha d\lambda \int \frac{dk}{2\pi}\Omega^n_{k,\lambda} \\ &= \int_0^\alpha d\lambda \int \frac{dk}{2\pi} i\left[\langle\partial_k u_n|\partial_\lambda u_n\rangle - \langle\partial_\lambda u_n|\partial_k u_n\rangle\right] \end{aligned} \tag{E8}$$

One can check the charge pumped across the unit cell is $c_1(2\pi) = -2e$ and $c_{2,3}(2\pi) = +e$.

[1] D. J. Thouless, Phys. Rev. B **27**, 6083 (1983).
[2] R. D. King-Smith and D. Vanderbilt, Phys. Rev. B **47**, 1651 (1993).
[3] D. Vanderbilt and R. D. King-Smith, Phys. Rev. B **48**, 4442 (1993).
[4] R. Resta, Rev. Mod. Phys. (1994).
[5] B. I. Sturman and P. J. Sturman, *Photovoltaic and Photorefractive Effects in Noncentrosymmetric Materials* (CRC Press, 1992).
[6] R. von Baltz and W. Kraut, Phys. Rev. B **23**, 5590 (1981).
[7] J. E. Sipe and A. I. Shkrebtii, Phys. Rev. B **61**, 5337 (2000).
[8] S. M. Young and A. M. Rappe, Phys. Rev. Lett. **109**, 116601 (2012).
[9] S. M. Young, F. Zheng, and A. M. Rappe, Phys. Rev. Lett. **109**, 236601 (2012).
[10] T. Morimoto and N. Nagaosa, Science Advances **2**, e1501524 (2016).
[11] L. Z. Tan, F. Zheng, S. M. Young, F. Wang, S. Liu, and A. M. Rappe, Npj Computational Materials (2016).
[12] F. Wang, S. M. Young, F. Zheng, I. Grinberg, and A. M. Rappe, "Bulk photovoltaic effect enhancement via electrostatic control in layered ferroelectrics," ArXiv:1503.00679 [cond-mat.mtrl-sci].
[13] I. Grinberg, D. V. West, M. Torres, G. Gou, D. M. Stein, L. Wu, G. Chen, E. M. Gallo, A. R. Akbashev, P. K. Davies, *et al.*, Nature **503**, 509 (2013).
[14] W. Nie, H. Tsai, R. Asadpour, J.-C. Blancon, A. J. Neukirch, G. Gupta, J. J. Crochet, M. Chhowalla, S. Tretiak, M. A. Alam, H.-L. Wang, and A. D. Mohite, Science **347**, 522 (2015).
[15] D. Shi, V. Adinolfi, R. Comin, M. Yuan, E. Alarousu, A. Buin, Y. Chen, S. Hoogland, A. Rothenberger, K. Katsiev, Y. Losovyj, X. Zhang, P. A. Dowben, O. F. Mo-

hammed, E. H. Sargent, and O. M. Bakr, Science **347**, 519 (2015).
[16] D. W. de Quilettes, S. M. Vorpahl, S. D. Stranks, H. Nagaoka, G. E. Eperon, M. E. Ziffer, H. J. Snaith, and D. S. Ginger, Science **348**, 683 (2015).
[17] L. C. Gomes, A. Carvalho, and A. H. Castro Neto, Phys. Rev. B **94**, 054103 (2016).
[18] M. Mehboudi, B. M. Fregoso, Y. Yang, W. Zhu, A. van der Zande, J. Ferrer, L. Bellaiche, P. Kumar, and S. Barraza-Lopez, Phys. Rev. Lett. **117**, 246802 (2016).
[19] G. G. Naumis, S. Barraza-Lopez, M. Oliva-Leyva, and H. Terrones, "A review of the electronic and optical properties of strained graphene and other similar 2d materials," (2016), arXiv:1611.08627 [cond-mat.mes-hall].
[20] C. Salazar, J. L. Cheng, and J. E. Sipe, Phys. Rev. B **93**, 075442 (2016).
[21] A. Zenkevich, Y. Matveyev, K. Maksimova, R. Gaynutdinov, A. Tolstikhina, and V. Fridkin, Phys. Rev. B **90**, 161409 (2014).
[22] A. M. Cook*, B. M. Fregoso*, F. de Juan, and J. E. Moore, Nat. Commun. **8**, 14176 (2017), (* Equal contributors).
[23] T. Rangel*, B. M. Fregoso*, B. S. Mendoza, T. Morimoto, J. E. Moore, and J. B. Neaton, "Giant bulk photovoltaic effect and spontaneous polarization of single-layer monochalcogenides," ArXiv:1610.06589 in press Phys. Rev. Lett. (* Equal contributors).
[24] R. M. Martin, *Electronic Structure: Basic Theory and Practical Methods* (Cambridge University Press, 2004).
[25] M. Lax, *Symmetry principles in solid state and molecular physics* (Dover publications, inc., 1974).
[26] M. J. Rice and E. J. Mele, Phys. Rev. Lett. **49**, 1455 (1982).
[27] K. Kushnir, M. Wang, P. D. Fitzgerald, K. J. Koski, and L. V. Titova, ACS Energy Letters **2**, 1429 (2017).
[28] K. Chang, J. Liu, H. Lin, N. Wang, K. Zhao, A. Zhang, F. Jin, Y. Zhong, X. Hu, W. Duan, Q. Zhang, L. Fu, Q.-K. Xue, X. Chen, and S.-H. Ji, Science (2016).